Negative-ion implantation into thin SiO2 layer for defined nanoparticle formation

AUTHOR(S):

Tsuji, H; Arai, N; Gotoh, N; Minotani, T; Ishibashi, T; Okumine, T; Adachi, K; Kotaki, H; Gotoh, Y; Ishikawa, J

CITATION:

Tsuji, H ...[et al]. Negative-ion implantation into thin SiO2 layer for defined nanoparticle formation. REVIEW OF SCIENTIFIC INSTRUMENTS 2006, 77(3): 03A510.

ISSUE DATE:

2006-03

URL:

http://hdl.handle.net/2433/39814

REVIEW OF SCIENTIFIC INSTRUMENTS **77**, 03A510 (2006)

Negative-ion implantation into thin SiO_2 layer for defined nanoparticle formation

Hiroshi Tsuji[a)]
Department of Electronic Science and Engineering, Kyoto University, Kyoto, Japan

Nobutoshi Arai
Department of Electronic Science and Engineering, Kyoto University, Kyoto, Japan and Devices Research Laboratory, SHARP Corporation, Tenri, Japan

Naoyuki Gotoh, Takashi Minotani, and Toyoji Ishibashi
Department of Electronic Science and Engineering, Kyoto University, Kyoto, Japan

Tetsuya Okumine, Kouichiro Adachi, and Hiroshi Kotaki
Devices Research Laboratory, SHARP Corporation, Tenri, Japan

Yasuhito Gotoh and Junzo Ishikawa
Department of Electronic Science and Engineering, Kyoto University, Kyoto, Japan

(Presented on 15 September 2005; published online 21 March 2006)

Two methods to form nanoparticles at a certain depth in a thin oxide layer by negative-ion implantation into the oxide layer of silicon substrate have been investigated. One method is by implantation at a low energy and the other is by a thermal diffusion after implantation. Regarding the low-energy implantation, about 1 keV of ion energy is required. In general, a surface charge-up of the oxide layer arises from a positive-ion implantation to affect ion penetration depth. In this research, we used negative ion implantation because of its advantage of almost "charge-up-free" feature, even for insulating materials. We obtained delta-layered gold nanoparticles (Au NPs) in a 25 nm thick SiO_2 layer on Si by the low-energy implantation method of gold negative ions at 1 keV. The center depth and an average diameter of the delta-layered Au NPs were 5 nm and 7 nm, respectively. As by the thermal diffusion after implantation, silver negative ions were implanted into 25 nm thick SiO_2/Si at 10 keV with 5×10^{15} ions/cm^2 at room temperature. Implanted atoms diffused from the implanted site, depending on annealing temperature. Only after annealing at 700 °C, delta-layered silver nanoparticles (Ag NPs) were obtained near the interface of SiO_2/Si.
 [DOI: 10.1063/1.2163287]

I. INTRODUCTION

Nanoparticle composite materials have many interesting features in optical and electrical properties. Especially, they show Coulomb blockade phenomena, even at room temperature. In the development of single electron devices with nanoparticles embedded in a thin oxide, such as the gate oxide layer of a metal-oxide-semiconductor field-effect transistor (MOSFET), nanoparticles with well-defined size and depth are required. Many researchers have tried to form delta-layered nanoparticles by using ion implantation.[1–6] The main purpose is to control the depth of implanted atoms in the ion-implantation method, which induces defects in the implanted region and thus requires a heat treatment for their recovery. Two methods considered are as follows: (1) ion implantation to the required depth for elements with a low thermal diffusion coefficient in SiO_2; and (2) rearrangement by heat treatment to control the depth of implanted atoms after implantation for metals with a relatively high diffusion coefficient. The former method requires a low-energy implantation to obtain a very shallow implanted depth with a narrow deviation for a very thin oxide layer such as a gate oxide. In this research, we used a negative-ion implantation that has an advantage of an almost "charge-up-free" feature in insulating materials.[7–9] It is expected to be suitable to nanoparticle formation in such a thin oxide layer with precise controls of the energy and dose amount. In this paper, we have investigated (1) the delta-layer formation of Au nanoparticles at a shallow depth in a SiO_2 layer by Au negative-ion implantation at a low energy; and (2) the delta-layer formation of Ag nanoparticles at a deep depth in the oxide layer near the boundary of SiO_2/Si by annealing subsequent to Ag negative-ion implantation.

II. RF SPUTTER-TYPE HEAVY NEGATIVE ION SOURCE AND NEGATIVE-ION IMPLANTER

Ion implantation of gold and silver negative ions in this research was performed by a negative-ion implanter (200 kV, Nissin Electric Corporation, Kyoto, Japan)[7,10] with our developed rf-plasma sputter-type negative-ion source.[11,12] Figure 1 shows a schematic diagram of the implanter, which consists of the plasma sputter-type negative-ion source, a magnetic mass separator, an acceleration col-

[a)]Author to whom correspondence should be addressed; electronic mail: tsuji@kuee.kyoto-u.ac.jp

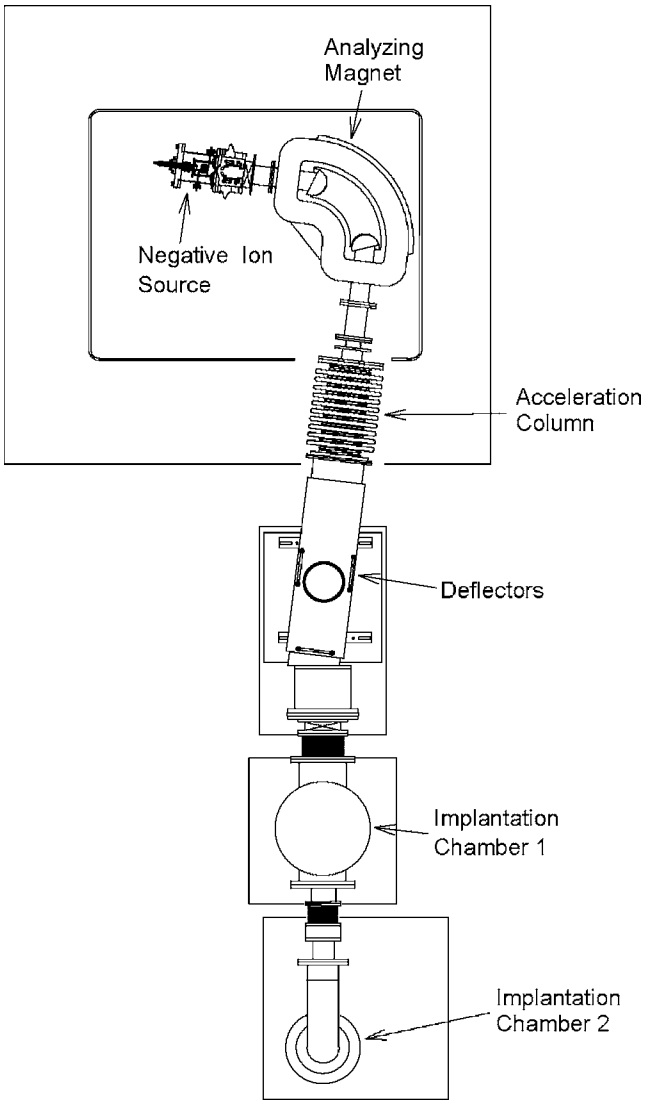

FIG. 1. Schematic diagram of a negative-ion implanter.

umn, a quadrupole lens, *X*-*Y* beam deflectors, a first implantation chamber with a horizontal beam (Chamber-1), a 90° electrostatic beam deflector, and a second chamber from a vertical direction (Chamber-2). The negative ion source as shown in Fig. 2 has a rf coil, a sputtering target of pure metal disk of gold or silver with 33 mm in diameter, and an exiting hole of negative ions. The rf discharge plasma of xenon gas was generated at first by feeding 13.56 MHz power of 100 W to the rf coil. Then, cesium vapor was delivered to the plasma. The target was negatively biased at 100–200 V negative to induce the bombardment of Xe and Cs positive ions on the target surface. A part of the sputtered particles of the target material came out from the surface as a negative ion. The negative ions were accelerated by the bias voltage and passed through the plasma. Then, they were extracted from the exit hole by an extraction electrode at 10–30 keV. Electrons in plasma and from the target were prevented by a magnetic field at the exit hole. After mass separation and acceleration, the negative-ion beam was deflected by 7° to eliminate fast neutrals resulting in the acceleration column. Finally, the transported negative-ion beam to a Faraday cup with a limiting hole of 8-mm diam in the implantation chamber (Chamber 1) entered onto a sample of a thin SiO_2 on Si substrate. For the implantation at a low energy less than the extraction energy, the negative-ion beam was decelerated in front of the Faraday cup. In this research, a relatively low current of about 0.5 μA (less than 1 $\mu A/cm^2$ in current density) was used to avoid unnecessary sample heating by the ion bombardment. The residual gas pressure during the implantation was less than 1×10^{-4} Pa.

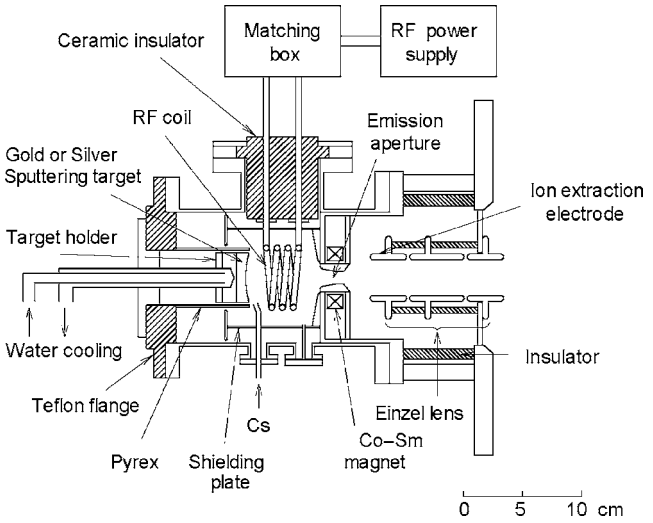

FIG. 2. Schematic diagram of a rf plasma-sputter-type heavy negative ion source.

III. DELTA-LAYER FORMATION OF Au NANOPARTICLES AT SHALLOW DEPTH

Mass-separated Au negative ions from a pure gold (99.999%) target were implanted to the thermally grown SiO_2 thin layer with thickness of 50, 25, and 10 nm on a Si substrate at an implantation energy of 35, 15, and 1 keV, respectively, at room temperature. The current density was within a range of 0.1–1 $\mu A/cm^2$. For the low-energy implantation at 1 keV, the Au negative-ion beam extracted at 15 keV was decelerated to 1 keV just before the Faraday cup. The energy was set as the implantation depth is expected to be a half the thickness of the oxide layer. The dose amount was 1×10^{16}, 5×10^{15}, and 2×10^{15} ions/cm^2 for

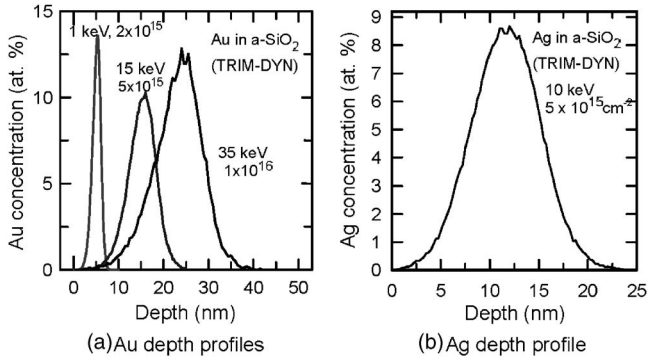

FIG. 3. Depth profiles of implanted metal atoms in amorphous SiO_2 medium calculated by using the TRI-DYN program: (a) for Au atoms at various conditions and (b) for Ag atoms at 10 keV with 5×10^{15} ions/cm^2.

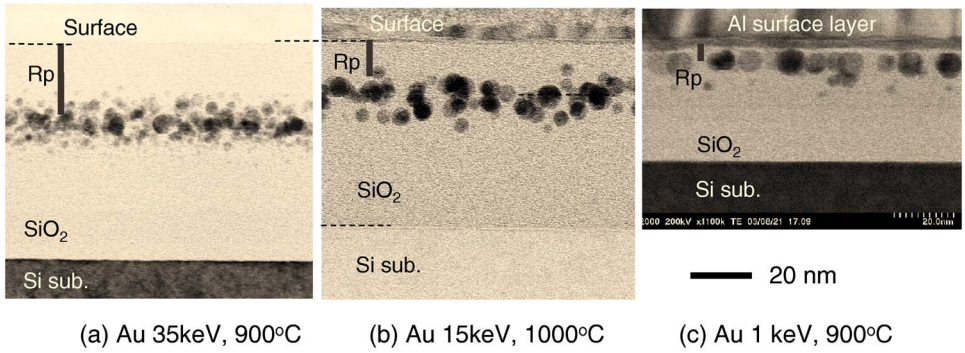

FIG. 4. X-TEM images of an Au-implanted oxide layer on a Si substrate: (a) implantation energy of 35 keV, dose of 1×10^{16} ions/cm^2, annealing temperature of 900 °C; (b) 15 keV, 5×10^{15} ions/cm^2, 1000 °C; and (c) 1 keV, 2×10^{15} ions/cm^2, 900 °C.

implantation at 35, 15, and 1 keV, respectively. The depth profiles of Au atoms in amorphous SiO_2 calculated by using the TRIM-DYN program[13] are shown in Fig. 3(a). These doses would make the peak concentration of Au atoms to be about 10 at. % for each case. After implantation, Au-implanted samples were annealed at 900 °C and 1000 °C for 1 h in 50 ml/min flow of Ar gas under decompression by a rotary pump. The size and distribution of created Au nanoparticles were observed by a cross-sectional transmission electron microscopy (X-TEM). The X-TEM samples were fabricated by a Ga focused ion beam apparatus (FB-2000, Hitachi Ltd.) and were observed by a scanning TEM apparatus (HD-2000, Hitachi Ltd.) with an electron beam at 200 keV. The X-TEM images of these three samples are shown in Fig. 4, where Au nanoparticles appeared in all of the three samples. In Fig. 4(a) at 35 keV implantation, Au nanoparticles of 2–6 nm in diameter formed in a wide depth range of 23 nm width around the center of 26 nm in depth. At 15 keV implantation, as shown in Fig. 4(b), Au nanoparticles of 3–7 nm in diameter formed with a relatively narrow distribution of 18 nm width at the center of 20 nm in depth. In the very low-energy implantation at 1 keV, as shown in Fig. 4(c), Au nanoparticles with almost the same size of 6–8 nm in diameter formed at the same depth of 5 nm in a single layer. This is almost a delta layer of Au nanoparticles, although a few small nanoparticles (~3 nm in diameter) were also found at a deeper position of 13 nm. The growth in the oxide layer was observed and the increment in thickness was about 20 nm for the three samples.

In the sample at 35 keV implantation and 900 °C annealing, the center depth of 26 nm in the wide particle distribution corresponded well to the calculated projected range, R_p, which is 25 nm. However, at 15 keV and 1000 °C, the center depth of 20 nm in the particle distribution was deeper than the calculated R_p of 12 nm. This is considered to be due to the thermal diffusion of implanted Au atoms. The Au atoms of nanoparticles were thermally diffused for the longer distance at the higher temperature, and thus the distribution moved to a deeper position due to 1000 °C. As for the very low-energy implantation at 1 keV, we obtained fairly good delta-layer formation of Au nanoparticles, although a few small nanoparticles formed at 13 nm depth. The reason for such deep and small Au nanoparticles is considered to be due to fast Au neutrals. Since an Au negative-ion beam was decelerated to 1 keV just before the Faraday cup, fast Au neutrals might have resulted in the collision of Au negative ions with residual gas particles and entered to the sample with the original energy of 15 keV. These fast neutrals might form the particles at a deeper site. As a result, a delta layer of nanoparticles is obtained by an implantation at low energy, giving a very narrow deviation of the implanted profile. The increase in thickness of SiO_2 is considered to be due to oxidation by residual gas in the annealing oven during the heat treatment with high temperature over 900 °C.

IV. DELTA-LAYER FORMATION OF Ag NPS AT DEEP DEPTH

Silver negative ions from a pure silver (99.99%) target after mass separation were implanted into a thermally grown 25 nm thick SiO_2 thin layer on a Si substrate at room temperature in the Faraday cup. The implantation conditions were at 10 keV of energy with 5×10^{15} ions/cm^2 of the dose amount by 0.4 μA/cm^2 of current density. The calculated depth profile of implanted Ag atoms is shown in Fig. 3(b). The profile was almost Gaussian distribution at a peak depth of about 12 nm with a peak concentration of 8.2 at. %. After implantation, samples were annealed at temperatures of 500 °C, 700 °C, and 800 °C in an Ar gas flow for 1 h.

The obtained X-TEM images after annealing at these temperatures are shown in Fig. 5. At a low annealing temperature of 500 °C in Fig. 5(a), relatively small Ag nanoparticles of 2–3 nm in diameter were formed in a wide depth in the SiO_2 layer. The number of particles was a few in the surface side shallower than 13 nm of R_p and a lot in the deeper just above the boundary to the Si substrate. At 700 °C, as shown in Fig. 5(b), Ag nanoparticles with almost the same size of 6 nm in diameter were observed to locate in one line at the same distance from the boundary to Si with the minimum distance of 2 nm. Such Ag nanoparticles disappeared from the SiO_2 layer at 800 °C, as demonstrated in Fig. 5(c). Thus, we obtained the delta layer of the Ag nano-

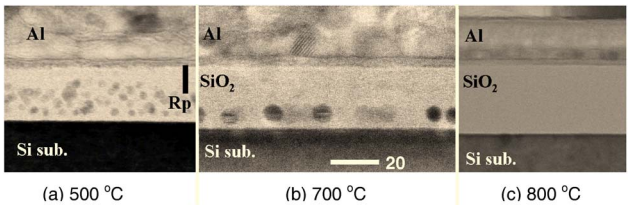

FIG. 5. X-TEM images of Ag-implanted 25 nm thick oxide layer on Si after annealing at various temperatures: (a) 500 °C; (b) 700 °C; and (c) 800 °C.

particles in the bottom region of the oxide film on Si. For the growth of the oxide layer, the increment in thickness of SiO_2 was only 2 nm at 700 °C and 4 nm at 800 °C.

The Ag nanoparticles were observed in the bottom region, much beyond the projected range of 13 nm, even at 500 °C. This is considered to be due to thermal diffusion. The Ag atoms diffused to the deeper position beyond their implanted sites and precipitated there as nanoparticles. On the contrary, Ag atoms diffused to the surface direction might detach from the surface after reaching the surface due to the large diffusion length in the shallower region, including many ion-induced defects rather than that in the deeper side without a defect. The Ag nanoparticles in the deepest layer at 500 °C are considered to align in one line just above the Si boundary with the distance of 2 nm like those at 700 °C. The Ag nanoparticles at 700 °C with the diameter larger than those at 500 °C finely aligned and made a delta layer at the minimum distance of 2 nm from the SiO_2/Si boundary. This result suggests the existence of a barrier that suppresses Ag atoms to diffuse onto the Si substrate. This barrier is considered to be due to the compressive stress in SiO_2 network just near the SiO_2/Si interface. The thermally grown SiO_2 is certainly amorphous. However, the transition region from the Si surface was affected by the regularity of Si crystal lattice, where oxygen atoms in SiO_2 were also bonded to the Si atoms in the Si crystal. Therefore, the compressive stress in the transition layer of SiO_2 was considered to suppress the Ag diffusion, resulting in an accumulation of the Ag atoms in front of the transition layer at 700 °C. The thickness of the transition layer is estimated to be about 2 nm.

V. CONCLUDING REMARKS

Two formation methods of delta-layered nanoparticles (NPs) of gold and silver in the thin dioxide layer on the Si substrate were studied by using negative-ion implantation and annealing. At a shallow depth, the delta-layered Au NPs were obtained by Au negative-ion implantation at a very low energy of 1 keV. This low-energy method can be applied to heavy metal with a low thermal mobility in SiO_2. At a deep depth, the delta-layered Ag NPs were also obtained by Ag negative-ion implantation with subsequent heat treatment. These techniques are considered to be important for development in single electron devices.

ACKNOWLEDGMENTS

The authors are grateful to Dr. Masayoshi Nagao and Miss Hiromi Yamauchi of the National Institute of Advanced Industrial Science and Technology (AIST), Tsukuba, for their assistance in the TEM observation.

[1] K. Yano, T. Ishii, T. Hashimoto, T. Kobayashi, F. Murai, and K. Seki, IEEE Trans. Educ. **41**, 1628 (1994).
[2] A. Nakajima, T. Futatsugi, N. Horiguchi, H. Nakao, and N. Yokoyama, Tech. Dig. - Int. Electron Devices Meet. **1997**, 159 (1997).
[3] H. Tsuji, N. Arai, T. Matsumoto, Y. Gotoh, and J. Ishikawa, Trans. Mater. Res. Soc. Jpn. **28**, l473 (2003).
[4] N. Kishimoto, N. Umeda, Y. Takeda, C. G. Lee, and V. T. Gritsyna, Nucl. Instrum. Methods Phys. Res. B **148**, 1017 (1999).
[5] A. Nakajima, T. Futatsugi, N. Horiguchi, and N. Yokoyama, Appl. Phys. Lett. **71**, 3652 (1997).
[6] H. Tsuji, N. Arai, T. Matsumoto, K. Ueno, Y. Gotoh, K. Adachi, H. Kotaki, and J. Ishikawa, Appl. Surf. Sci. **238**, 132 (2004).
[7] J. Ishikawa, H. Tsuji, Y. Toyota, Y. Gotoh, K. Matsuda, T. Tanjo, and S. Sasaki, Nucl. Instrum. Methods Phys. Res. B **96**, 7 (1995).
[8] H. Tsuji, Y. Toyota, J. Ishikawa, S. Sasaki, Y. Okayama, S. Nagumo, Y. Gotoh, and K. Matsuda, *Ion Implantation Technology-94* (Elsevier, New York, 1995), p. 612.
[9] H. Tsuji, Y. Gotoh, and J. Ishikawa, Nucl. Instrum. Methods Phys. Res. B **141**, 645 (1998).
[10] H. Tsuji and J. Ishikawa, Rev. Sci. Instrum. **63**, 2488 (1992).
[11] H. Tsuji, J. Ishikawa, Y. Gotoh, and Y. Okada, AIP Conf. Proc. **287**, 530 (1994).
[12] H. Tsuji, S. Kido, H. Sasaki, Y. Gotoh, and J. Ishikawa, Rev. Sci. Instrum. **71**, 804 (2000).
[13] J. P. Biersack, Nucl. Instrum. Methods Phys. Res. B **27**, 21 (1987).